Thermodynamic Studies of Anion Adsorption at Stepped Platinum(*hkl*) Electrode Surfaces in Sulfuric Acid Solutions

Jorge Mostany,[†,‡] Enrique Herrero,[†] Juan M. Feliu,*[,†] and Jacek Lipkowski*[,†,§]

Departamento de Química Física, Universidad de Alicante, Apart 99, E−03080 Alicante, Spain, Departamento de Química, Universidad Simón Bolívar, Apartado 89.000, Caracas 1080-A, Venezuela, and Department of Chemistry and Biochemistry, University of Guelph, Guelph, Ontario N1G 2W1, Canada

Received: July 18, 2002; In Final Form: September 27, 2002

The thermodynamics of the so-called perfectly polarized electrode was employed to analyze the total charge densities for stepped Pt(*hkl*) electrodes in solutions of H_2SO_4 with an excess of an inert electrolyte (0.1 M $HClO_4$). Three Pt single-crystal electrodes—Pt(10,10,9) = 20(111)×(111), Pt(7,7,6) = 14(111)×(111), and Pt(5,5,4) = 10(111)×(111)—vicinal to the Pt(111) surface were employed in these studies. A complete thermodynamic analysis using the electrode potential and the charge as independent variables has been performed. The Gibbs excess, Gibbs energy of adsorption, electrosorption valency, and Esin−Markov coefficients for (bi)sulfate adsorption at these surfaces have been determined. The thermodynamic data display a dependence on the crystallographic structure of the Pt electrode surface. Both the Gibbs excess and the Gibbs energy of adsorption decrease with increasing step density or decreasing terrace length. This result indicates that adsorption of (bi)sulfate is stronger at larger (111) terraces.

1. Introduction

There is a growing interest in using stepped surfaces to study coordination phenomena at electrified interfaces. These electrodes are particularly useful to elucidate the influence of the long-range order and the number and symmetry of step sites on the reactivity of electrode surfaces. For example, it has been shown that in some situations, "ideal" two-dimensionally ordered surfaces such as Pt(111) are inactive for CO oxidation[1,2] and that defect sites are need for the reaction to proceed.

Numerous studies demonstrated that the electrochemical reactivity of a Pt electrode is related to the presence of wide two-dimensional surface domains. The presence of such domains is directly related to the pretreatment of the electrode, usually the flame annealing procedure,[3−6] and their effect on the electrochemical reactivity has been shown in the case of metal underpotential deposition reaction either at intermediate coverages, where anion coadsorption plays a key role in the building of the adlayer,[7] or in the formation of well-ordered metal fully covered monolayers.[8]

The sharp spike observed in voltammetric profile of the Pt(111) electrode in sulfuric acid containing solutions constitutes the best known example of the influence of the long-range order of the electrode surface on anion adsorption phenomena.[9] This sharp spike is very sensitive to the existence of wide (111) terraces. A number of articles have been devoted to voltammetric behavior of stepped electrodes having (111) terraces and monatomic steps with (111) or (100) orientation.[10−13] These stepped surfaces may be denoted as Pt(S)[*n*(111)×(111)], with Miller indices indicated by Pt(*n*,*n*,*n*−2), or Pt(S)[*n*(111)×(100)] having Miller indices described by Pt(*n*+1,*n*−1,*n*−1), where *n* is the number of terrace atoms. The voltammetric studies have pointed out that both hydrogen and anion adsorption strongly depends on the step density of the electrode.[12,14]

Integration of cyclic voltammograms is frequently used to determine the amount of adsorbates at the electrode surface. Despite its importance, this procedure gives only the total charge and further experiments are required to discriminate between hydrogen and anion contributions to the measured total charge. Among them, CO displacement has been used to determine whether the total charge on the electrode at a fixed potential corresponds to adsorption of the anion or the cation.[15] As an alternative strategy, we have recently shown that thermodynamics of the perfect polarized electrode may be used to analyze the total charge density data and that Gibbs excesses and Gibbs energies of (bi)sulfate adsorbed at a Pt(111) surface may be determined in that way.[16]

In the present paper, we will use the thermodynamic approach to gain quantitative insight into (bi)sulfate adsorption on three stepped surfaces in the series Pt(S)[(*n*)(111)×(111)]. These surfaces consist of relatively long (111) terraces and monatomic steps and can be denoted using Miller notation as Pt(10,10,9) (*n* = 20), Pt(7,7,6) (*n* = 14) and Pt(5,5,4) (*n* = 10). Taking into account that (110) steps are formed at the junction between the (111) terrace and the (111) step,[11] they may also be described as Pt(S)[(*n*−1)(111)×(110)]. In fact, CV studies of hydrogen adsorption at these surfaces demonstrated that an adsorption state, linked to the steps, appears at 0.12 V. Hydrogen adsorption at Pt(110) takes place at the same potential. This behavior suggests that the new adsorption state at the stepped surfaces is due to the presence of (110) sites. The potentials of the zero total charge (PZTC) have been determined for these electrodes. Their values depend linearly on the step density,[15] indicating that indeed the structure of these surfaces may be represented as a linear combination of terrace and step sites, indeed. It has also been shown that topography of these surfaces imaged by STM is in good agreement with the topography predicted from their nominal crystallographic orientation.[14]

Several questions concerning (bi)sulfate adsorption on these surfaces remain unsolved, namely (i) at which potentials anion

[†] Universidad de Alicante.
[‡] Universidad Simón Bolívar.
[§] University of Guelph.

10.1021/jp026561p CCC: $22.00
Published on Web 11/14/2002

adsorption takes place at steps and at which at terraces, (ii) how surface excesses and Gibbs energies depend on the step density and (iii) how the competitive adsorption of OH affects the (bi)-sulfate adsorption.[17] Some indirect evidence suggests that the so-called unusual adsorption states at intermediate potentials (between 0.45 and 0.8 V) are linked only to anion adsorption on terraces.[18] The use of electrodes with long terraces should allow us to determine whether bisulfate is preferentially adsorbed at terraces or at steps. This study should shed light on the role of surface defects on the (bi)sulfate adsorption at a Pt electrode.

2. Experimental Section

The electrochemical experiments were performed using Pt single-crystal beads oriented, cut and polished at 2.79, 4.04, and 5.77° from the [111] plane in the [1$\bar{1}$0] crystallographic zone, to expose the (10,10,9), (7,7,6), and (5,5,4) crystalline faces, characterized by terraces 20, 14, and 10 atoms wide separated by monatomic (111) steps. The corresponding electrode areas were 3.99, 3.89, and 2.79 mm^2. In all cases, electrodes were annealed in a propane/air flame, cooled in H_2 + Ar atmosphere and quenched with water in equilibrium with this reductive atmosphere, as described in ref 12.

Milli-Q water (18 MΩ cm resistivity) was used to rinse the cell and to prepare solutions. The perchloric and sulfuric acid solutions were prepared from Merck Suprapure Reagents. 0.1 M $HClO_4$ was used as supporting electrolyte, in which 13 different sulfuric acid concentrations were added in the range from 10^{-4} to 10^{-2} M to determine the Gibbs excess of adsorbed (bi)sulfate. The solutions had the following composition; 0.1 M $HClO_4$ + x M H_2SO_4, with $x = 0$, 1×10^{-4}, 1.25×10^{-4}, 2.5×10^{-4}, 3.75×10^{-4}, 5×10^{-4}, 7.5×10^{-4}, 1×10^{-3}, 1.5×10^{-3}, 2.5×10^{-3}, 3.75×10^{-3}, 5×10^{-3}, 7.5×10^{-3}, and 1×10^{-2} M. The electrolytes were purged with argon, and the solution was kept under the argon blanket throughout the duration of the experiment.

An all glass cell, a hydrogen reversible electrode (RHE) as a reference electrode and a large area platinum counter electrode were used to perform experiments. The electrochemical experiments were performed using the Autolab model PGSTAT 30 potentiostat controlled by a computer. The numerical treatment of the data has been performed with software packages Microcal Origin 6.1 and Mathcad Professional 2001. All measurements were conducted at a room temperature of 20 ± 2 °C

3. Results and Discussion

3.1. Cyclic Voltammetry and Charge Density Plots. Cyclic voltammetry (CV) was employed to determine the charge density at the Pt(*hkl*) electrode surface for further thermodynamic data analysis. Parts a−c of Figure 1 show CVs determined in solutions of perchloric acid, both pure and with addition of H_2SO_4, for the three Pt(*hkl*) surfaces. To avoid contamination and to ensure good reproducibility, all curves were recorded during a period of few hours. The concentration of sulfuric acid was progressively increased by spiking the 0.1 M $HClO_4$ supporting electrolyte with a concentrated solution of H_2SO_4. Within the hydrogen UPD region (at $E < 0.4$ V), the curves recorded in different sulfuric acid solutions overlap nicely with the reference curve recorded in the pure 0.1 M $HClO_4$. This feature indicates an excellent reproducibility and proves that oxygen content in the electrolyte is low. It is worth mentioning that the position and shape of the peak appearing at 0.125 V is insensitive to the sulfuric acid concentration, even at concentrations as high as 0.5 M H_2SO_4.[15] This fact clearly indicates that only hydrogen adsorption/desorption on the step are responsible

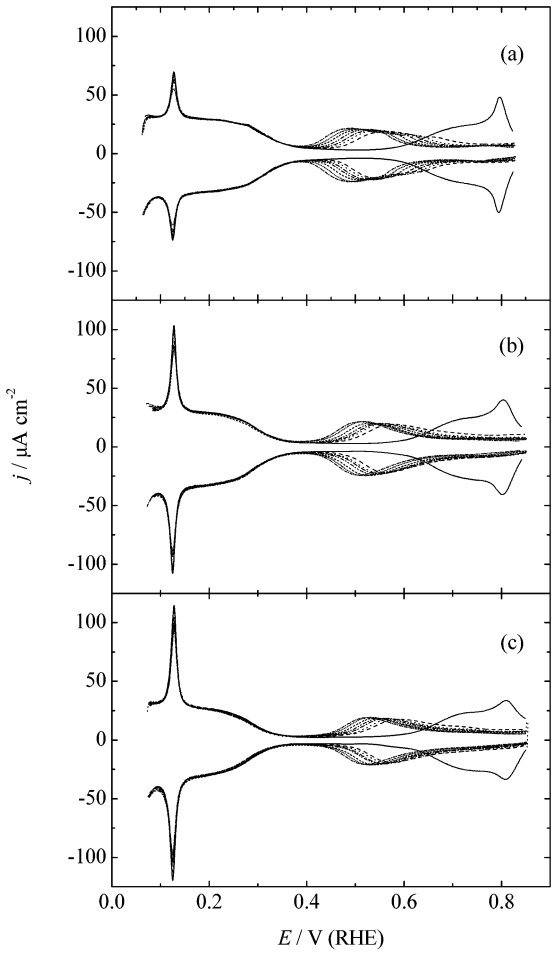

Figure 1. Cyclic voltammograms for (a) Pt(10,10,9), (b) Pt(7,7,6), and (c) Pt(5,5,4) electrodes in 0.1 M $HClO_4$ + x M H_2SO_4 solutions with x equal to 0, 1.0×10^{-4}, 2.5×10^{-4}, 5×10^{-4}, 1.0×10^{-3}, 2.5×10^{-3}, 5.0×10^{-3}, and 1.0×10^{-2} M. Sweep rate = 50 mV s^{-1}. Potentials measured vs RHE.

for this voltammetric feature. Similar conclusions were reached earlier in classical papers by Clavilier et al. dealing with the charge analysis of the whole of the stepped surfaces in the same crystallographic zone [11,19,20]

At $E > 0.4$ V, CVs recorded in the pure 0.1 M $HClO_4$ and in H_2SO_4 solutions differ significantly. In the presence of H_2SO_4, CVs display a characteristic broad pseudocapacity maximum at $E \sim 0.5$ V. The maximum shifts in the negative direction when the bulk concentration of sulfuric acid increases. For concentrations higher than 2.5×10^{-4} M, the sections of CVs recorded during positive (adsorption) and negative (desorption) voltage sweeps are symmetric indicating the reversibility of the (bi)sulfate adsorption/desorption process. For the two lowest concentrations of sulfuric acid, the CVs are not so symmetric, indicating certain degree of irreversibility caused by a slow mass transport in these rather diluted solutions.

For 0.1 M $HClO_4$ + 1 mM H_2SO_4 solution, parts a and b of Figure 2 compare the CVs for the three vicinal surfaces to the CV recorded at a Pt(111) electrode. Clearly, the well-defined peak at $E = 0.125$ V, seen on CVs recorded for the vicinal surfaces can be assigned to hydrogen adsorption at the step sites.[12,15] The presence of steps has a profound effect on (bi)-sulfate adsorption. The sharp spike seen at $E \sim 0.6$ V for the Pt(111) surface, corresponding to the phase transition between ordered and disordered state of adsorbed (bi)sulfate,[12,15,21] is barely visible at the Pt(10,10,9) plane that has 20 atoms wide

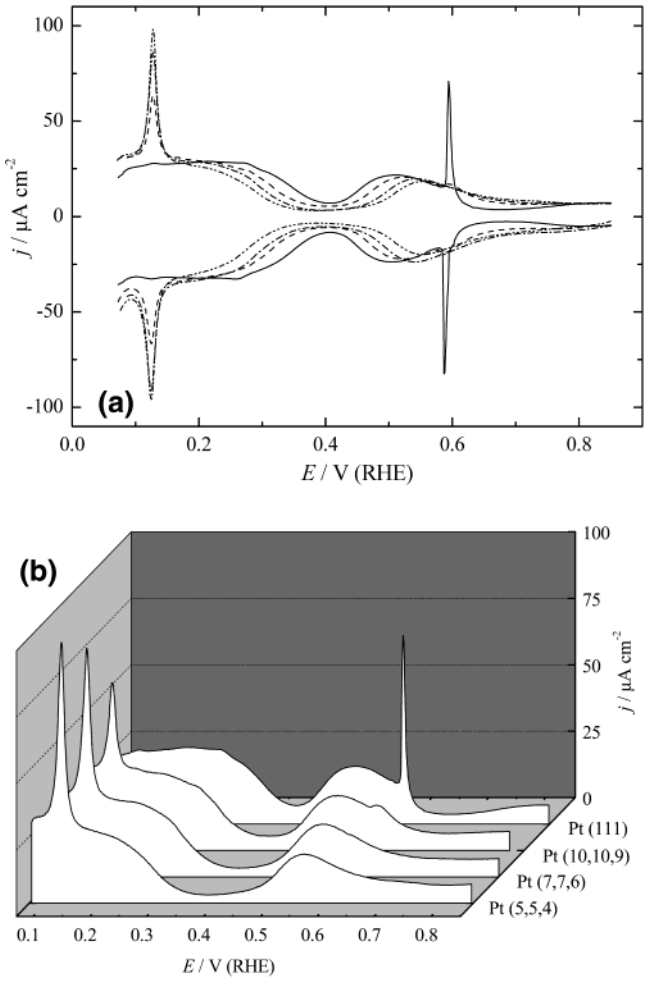

Figure 2. (a) Cyclic voltammograms for (—) Pt(1,1,1), (- - -) Pt(10,10,9), (— • —) Pt(7,7,6) and (— •• —) Pt(5,5,4) electrodes in 0.1 M $HClO_4$ + 1.0 mM H_2SO_4 solutions. (b) Positive direction of cyclic voltammograms shown in part a. Sweep rate 50 mV s^{-1}. Potentials were measured vs RHE.

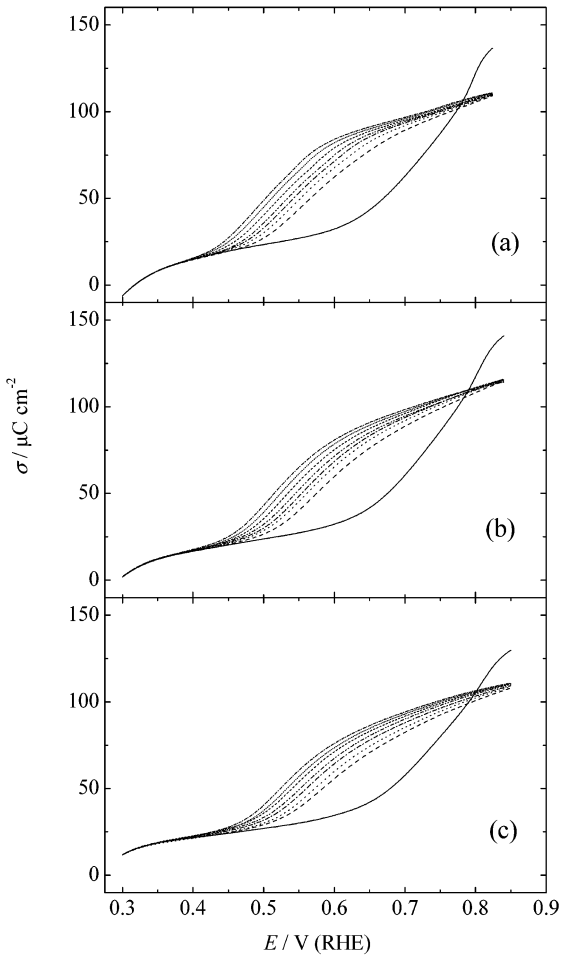

Figure 3. Charge density curves: (a) Pt(10,10,9), (b) Pt(7,7,6), and (c) Pt(5,5,4) electrodes in 0.1 M $HClO_4$ + *x* M H_2SO_4 solutions with *x* equal to 0, 1.0×10^{-4}, 2.5×10^{-4}, 5×10^{-4}, 1.0×10^{-3}, 2.5×10^{-3}, 5.0×10^{-3}, and 1.0×10^{-2} M (from left to right). Potentials were measured vs RHE.

(111) terraces. It disappears from CVs recorded for Pt(7,7,6) and Pt(5,5,4) with much narrower terraces. Clearly, the correlation length of the ordered phase is much higher than the width of terraces at the vicinal surfaces. Overall, parts a and b of Figure 2 show that when the terrace width decreases, the hydrogen adsorption shifts to negative potentials while (bi)sulfate adsorption shifts to positive potential. As a result, the adsorption of hydrogen and (bi)sulfate are better separated at the electrodes with higher step density.

The CVs reported in this section were integrated to determine the primary piece of information, the total charge density at the electrode surface (σ). The following potentials of the zero total charge (PZTC) for the pure 0.1 M $HClO_4$ solution—Pt(10,10,9), 317 mV; Pt(7,7,6), 293 mV; Pt(5,5,4), 261 mV (RHE)—determined with the help of the CO displacement method,[15,21] were used as the integration constants. In addition, it was assumed that at $E = 0.3$ V, where CVs for the sulfuric acid solutions merge with the CV for the pure electrolyte, (bi)sulfate ions are totally desorbed from the electrode surface and charge densities are independent of the presence of sulfuric acid in the mixed electrolyte. Because the CV curves were symmetric, the charge curve was the result of averaging of the charge obtained by integration of the voltammetric curves recorded in positive and negative potential scans. For the two lowest concentrations, a visual inspection of CVs in Figure 1 shows that the section recorded during the voltage sweep in positive direction is more distorted by slow mass transport than the section recorded when the potential is swept in negative direction. Therefore, sections of CVs corresponding to the voltage sweep in negative direction were taken for the charge density calculation.

The σ vs potential plots, calculated by integration of CVs, are shown in parts a—c of Figure 3 for several sulfuric acid concentrations. At potentials lower than 0.4 V, the curves determined for different solutions merge into a single line. That important feature indicates an excellent reproducibility of the experimental conditions throughout the whole series of measurements. At potentials more positive than 0.4 V a characteristic step corresponding to adsorption of (bi)sulfate appears on the charge density plot. The changes of charge are rather gradual. The charge density curves for all sulfuric acid solutions merge at $E \sim 0.7$ V to form a quasi-plateau. They intersect the curve of the supporting electrolyte at $E \sim 0.78$ V. The charge density plots in Figure 3, parts a—c, constitute the basic experimental data from which the Gibbs excess of adsorbed (bi)sulfate was calculated. The procedure described in [16,22] has been used in further data analysis.

3.2. Gibbs Excess Data. Integration of the charge potential plots allows to calculate surface pressure due to adsorbed anion $\Phi = \gamma_{\theta=0} - \gamma_\theta$:[16,22]

$$\Phi = \int_{E_{\theta=0}}^{E_\theta} (\sigma_\theta - \sigma_{\theta=0})\, \mathrm{d}E \qquad (1)$$

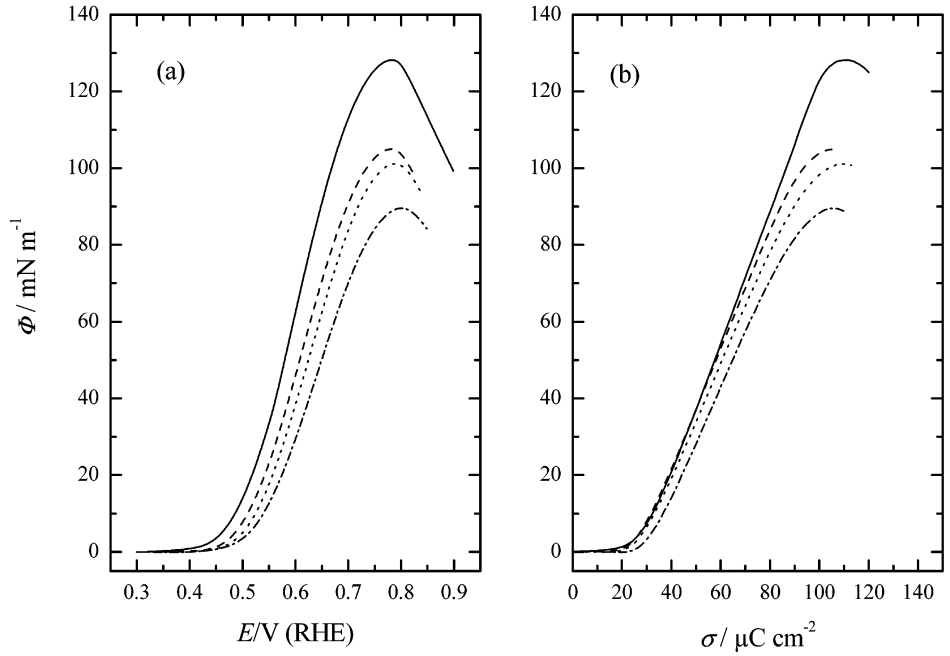

Figure 4. (a) Surface pressure Φ, measured at constant potential vs E and (b) Φ at constant charge vs σ plots for (—) Pt(1,1,1), (- - -) Pt(10,10,9), (···) Pt(7,7,6), and (— · —) Pt(5,5,4) electrodes in 0.1 M $HClO_4$ + 5.0 mM H_2SO_4 solutions.

where γ is the surface energy and subscripts $\theta = 0$ and θ denote the values of the surface energy and the difference of the total charge density measured in pure 0.1 M $HClO_4$ and 0.1 M $HClO_4$ + x M H_2SO_4 solutions, respectively. Independently, with the help of the Parsons function $\xi = \sigma_M E + \gamma$ one can calculate the surface pressure at constant charge using the following equation:[23]

$$\Phi = \xi_{\theta=0} - \xi_{\theta} = \int_{\sigma_{\theta=0}}^{\sigma} (E_{\theta=0} - E_{\theta})\, d\sigma \qquad (2)$$

Representative surface pressure vs potential or charge plots are shown in Figure 4, parts a and b, respectively. For the sake of comparison, surface pressure curves for the Pt(111) surface, taken from our previous work,[16] are also included in these figures. The surface pressures at either constant potential or charge display a maximum when plotted against the corresponding electrical variable. The maximum is observed at σ and E where in Figure 2 the charge density curve for pure 0.1 M $HClO_4$ electrolyte intersects the curves for the sulfuric acid solutions. These coordinates are the charge σ_{max} and the potential E_{max} of maximum adsorption, respectively. Apparently, E_{max} shifts somewhat to higher potentials and σ_{max} to somewhat lower charge densities when the step density at the Pt(*hkl*) surface increases. More significantly, the film pressures progressively decrease by moving from (111) to (5,5,4) surface, indicating that (bi)sulfate adsorption at stepped surfaces is weaker than at the (111) surface.

The Gibbs excess Γ_- of adsorbed anion was subsequently determined by differentiating the film pressure with respect to $\mu_{H_2SO_4}$ either at constant potential or at constant charge, as described in refs 16 and 22. We note that the thermodynamic analysis carried out in solutions of a constant pH cannot identify the nature of the predominantly adsorbed anion and, as in the previous papers [16,22,24], the measured quantity will be reported as the sum of the two surface species $\Gamma_- = \Gamma_{HSO_4^-} + \Gamma_{SO_4^{2-}}$ with $\Gamma_{HSO_4^-}$ and $\Gamma_{SO_4^{2-}}$ being the Gibbs excess of bisulfate and sulfate, respectively.

For Pt(5,5,4) surface with the highest step density, Figure 5a plots the surface excess vs the electrode potential determined using potential as the independent electrical variable. Inset to Figure 5b shows the dependence of the Gibbs surface excess vs charge calculated using charge as the independent electrical variable. The Gibbs surface excess vs charge plot is virtually independent of the bulk sulfuric acid concentration. Hence, only one curve is shown in the inset. For purpose of comparison with the data in Figure 5a, the charge vs potential curves, presented earlier in Figure 3c, were used to convert the Gibbs excesses vs charge plot shown in the inset to Figure 5b, into a dependence of Γ_- on the electrode potential. These data are shown in the main section of Figure 5b. A brief inspection of Figure 5, parts a and b, reveals that the analysis at a constant potential and at a constant charge give quite similar result. However, for consistency with the previously reported studies of bisulfate adsorption at the Pt(111) electrode surface, further data analysis will be based on the results presented in Figure 5b, determined from the analysis carried out using charge as the independent electrical variable.

For Pt(10,10,9) and Pt(7,7,6), insets to Figure 6, parts a and b, show the Gibbs excess vs charge density plots determined from the constant charge analysis. These data combined with charge density curves presented in Figure 3, parts a and b, were used to construct the Gibbs excess vs the electrode potential plots displayed in the main section of Figure 6, parts a and b. In general, the Gibbs excess data presented in Figure 5b and Figure 6, parts a and b, show that Γ_- decreases and the Γ_- vs E curves shift somewhat in the positive direction when the terrace width on the vicinal surfaces decreases.

This trend may conveniently be seen in Figure 7 which compares the Gibbs excess vs potential (part a) and charge (part b) plots determined for the three vicinal surfaces and the Pt(111) plane in 5 mM H_2SO_4. As aforementioned, the Gibbs excess at constant potential diminishes with increasing step density. The observed changes are larger than the experimental error, estimated as ±3%, indicating that the thermodynamic method is capable of discerning the effects of the step density on the (bi)sulfate adsorption process. The Gibbs excess at constant charge is very weakly dependent on the bulk concentration and these data represent the coverage averaged over the

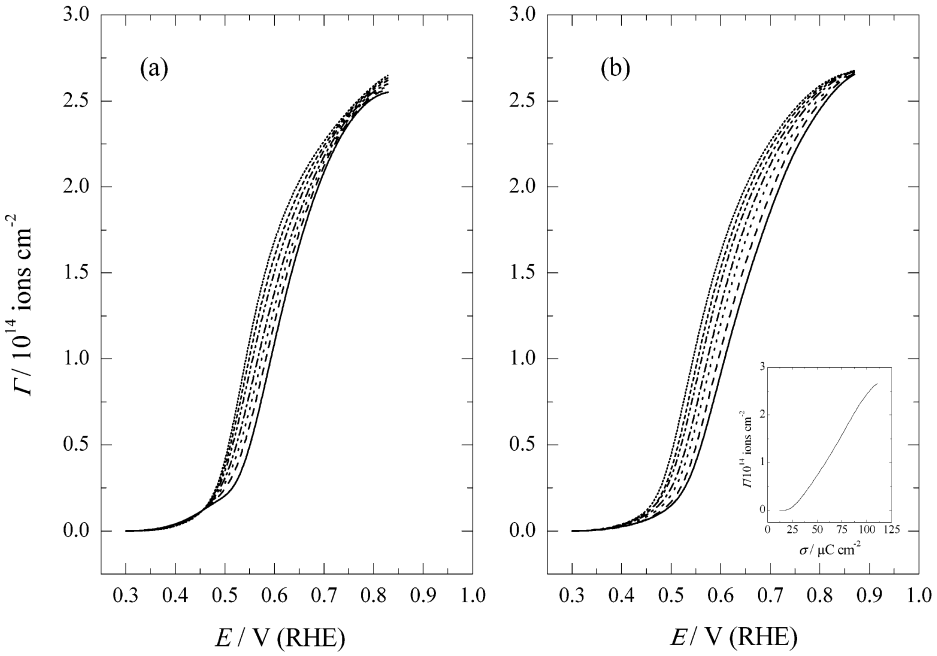

Figure 5. Gibbs excess Γ_-, determined from (a) analysis at constant potential and (b) constant charge vs E plots, for the Pt(5,5,4) electrode obtained in the solutions described in Figure 1. Inset shows the corresponding Γ_- vs σ plot.

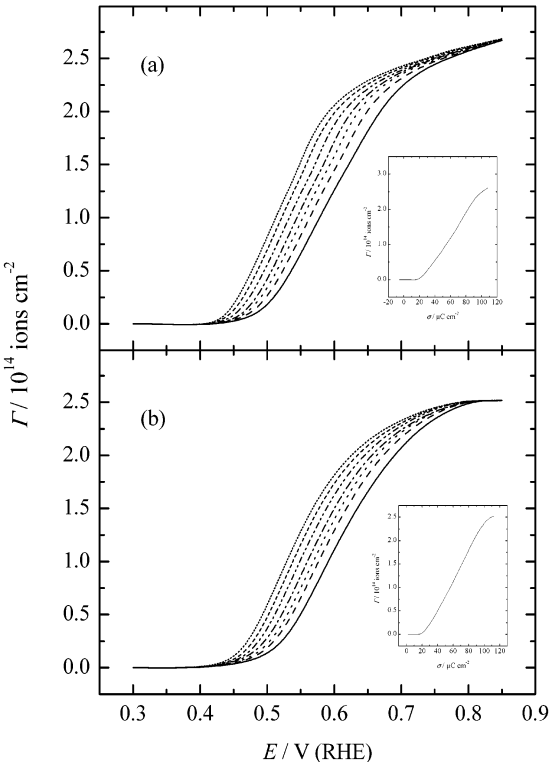

Figure 6. Γ_- vs E for the (a) Pt(10,10,9) and (b) Pt(7,7,6) surfaces with Γ_- data from the analysis at constant charge. Insets shows the corresponding Γ_- vs σ plots.

whole range of bulk sulfuric acid concentrations. Here, the rising sections of the curves almost overlap and the effect of the surface crystallography is seen only at the limiting surface concentrations. Interestingly, when charge is used as the electrical variable, the Gibbs excess data depend much less on both the bulk sulfuric acid concentration and the crystallographic orientation.

STM studies of the Pt(10,10,9) surfaces after different cooling conditions [14] have shown that after Ar + H_2 treatment, regular step-terraces patterns are observed, with a terrace width of ~4.6 nm, corresponding to the step density of 2.17×10^6 cm^{-1}. Similar experiments performed with Pt(7,7,6) and Pt(5,5,4) surfaces yielded step densities 3.11×10^6 and 4.46×10^6 cm^{-1} respectively. It has also been shown that the potential of zero total charge (PZTC) of stepped Pt surfaces depends in a linear fashion on the step density, for values of n_s as high as 10×10^6 cm^{-1}.[17,21] In Figure 8a, for selected potentials, the Gibbs excess is plotted against the step density n_s. Although each plot contains only three data points, one is tempted to assume that the concentration of adsorbed anion linearly decreases with the step density. One can also extrapolate these linear plots to zero step density. For the highest and the lowest bulk H_2SO_4 concentration, Figure 8b compares the Gibbs excess at "zero step density", calculated by a linear extrapolation of Γ_- vs n_s plots, with the Gibbs excesses determined for the Pt(111) surface. Below the phase transition potential, the agreement between the extrapolated and experimental data is quite good. At potentials more positive than the phase transition potential, the agreement is poor since the ordered phase does not exist at the stepped surfaces.

3.3. Gibbs Energies of Adsorption. Consistent with previous studies of (bi)sulfate adsorption at the Au(111) and Pt(111) surfaces,[16,22] the Gibbs energies of adsorption were calculated by fitting the surface pressure data to an equation of a " square root " isotherm:[25]

$$\ln(kTc_{H_2SO_4}) + \ln \beta = \ln \Phi + B\Phi^{1/2} \qquad (3)$$

where $\beta = \exp[-\Delta G/kT]$ is the adsorption equilibrium constant, B is a constant and Φ is the surface pressure. Figure 9a shows the plots of the square-root of the surface pressure vs $\ln(kTc_{H_2SO_4}/\Phi)$ for the analysis carried out at constant potential for the Pt(5,5,4) electrode. Figure 9b shows a similar analysis carried out at a constant charge density. The plots are somewhat wavy, however they were fit to a linear regression, which by extrapolation to zero surface pressure gave an intercept with the $\ln(kTc_{H_2SO_4}/\Phi)$ axis (abscissa at the origin) equal to

$$\lim_{\Phi \to 0} \ln(kTc_{H_2SO_4}/\Phi) = -\ln\beta \qquad (4)$$

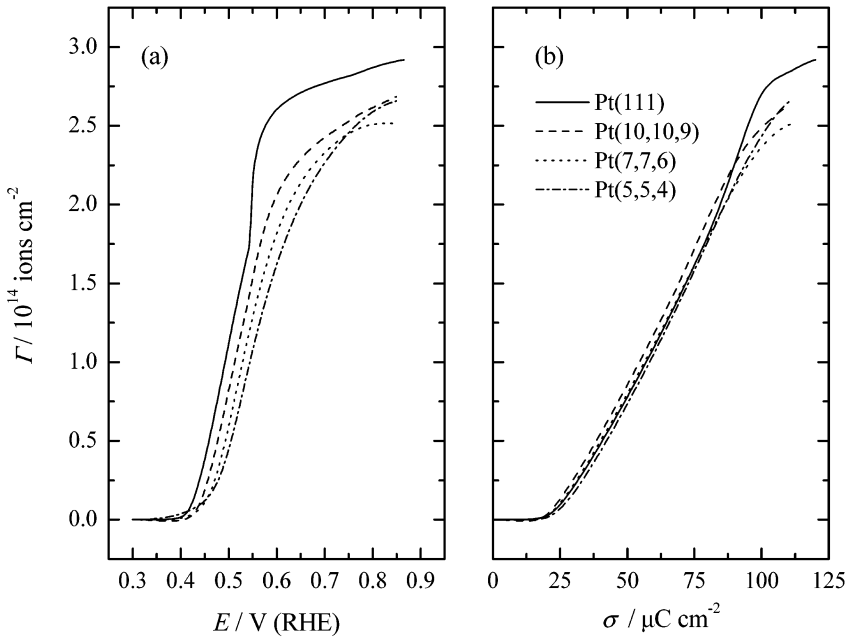

Figure 7. Comparison of the Gibbs excess vs potential plots, determined for the four Pt(*hkl*) surfaces from 0.1 M $HClO_4$ + 5.0 mM H_2SO_4 solutions. (b) Comparison of the Gibbs excess vs total charge density plots for the four Pt(*hkl*) surfaces: solid line, Pt(111); dashed line, Pt(10,10,9); dotted line, Pt(776); dotted and dashed line, Pt(554).

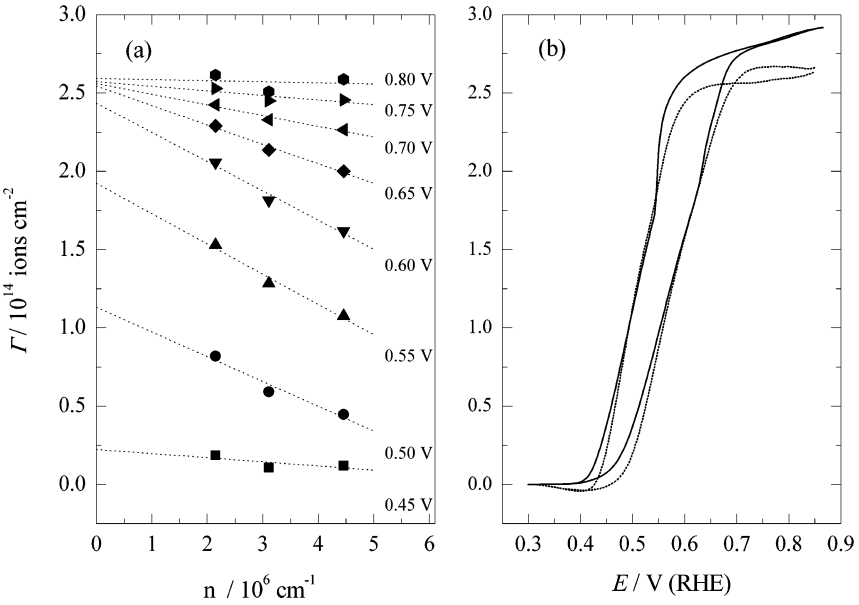

Figure 8. (a) Extrapolation of Gibbs excesses to zero step density and (b) comparison with the Γ_- vs E plot for Pt(1,1,1) for the more dilute and concentrated H_2SO_4 solutions.

The Gibbs energies of adsorption were then calculated from the intercept. In Figure 9, parts a and b, the sulfate concentrations are multiplied by the *kT* term so that in the limit of low coverages the film pressure is described by Henry's law $\Phi = kT\beta c_{H_2SO_4}$ as explained in ref 16 and 22. We would like to emphasize that for Pt(111) surface described in the previous paper[16] and for the two other vicinal surfaces, the fit of the surface pressure data to eq 3 was much better than for the Pt(5,5,4) surface. Therefore, the fit shown in Figure 9, parts a and b, may be considered as the worst case.

The Gibbs energies of adsorption, determined in that way, are plotted against potential and charge in Figure 10, parts a and b, respectively. Apparently, they vary in a quasi-parabolic fashion with the electrical variable. The standard state is an "ideal" $\Gamma = 1$ molecules cm^{-2} for the surface species and an "ideal" $c_{H_2SO_4} = 1$ mol dm^{-3} for the bulk species.[16,22] There is an overall good agreement between Gibbs energies determined using *E* and σ as the electrical variable. When potential is used as the electrical variable, the position of the minimum on the Gibbs energy plot coincides with the position of the maximum on the surface pressure plot shown in Figure 4a. The minimum on the Gibbs energy plots calculated at constant charge is observed at somewhat lower σ than the value corresponding to the maximum on the surface pressure plots in Figure 4b. This may indicate that Gibbs energies at constant charge are affected by a certain systematic error of the long extrapolation procedure. However, as shown in Figure 10b, the error bars for the Gibbs energies of adsorption indicate an uncertainty varying from ±12% at the onset of adsorption where charge values are rather small (less than 20 μC cm^{-2}), to ±5%

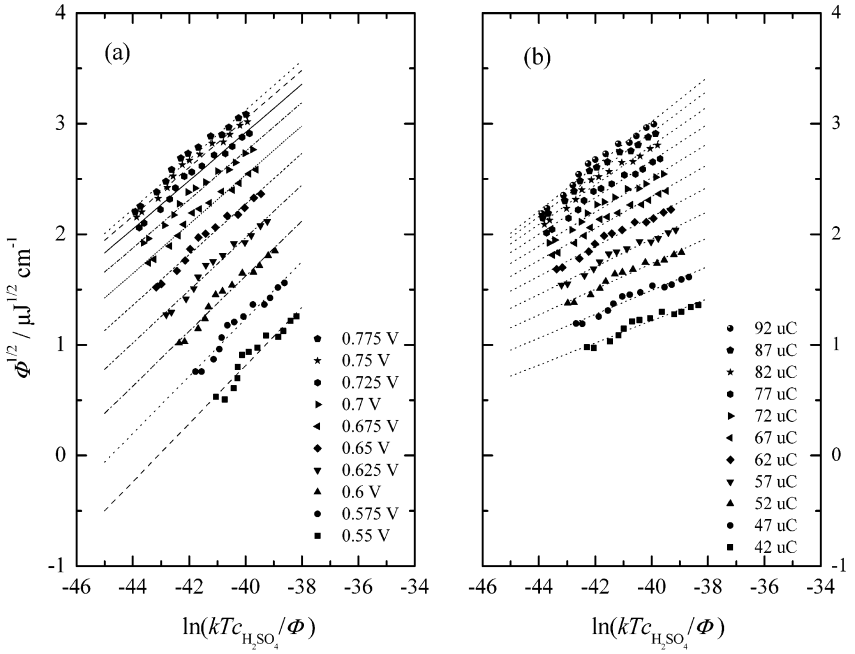

Figure 9. Fit of the surface pressure data Φ to the square root isotherm for the Pt(5,5,4) electrode obtained with (a) *E* and (b) *σ* as the independent electrical variable.

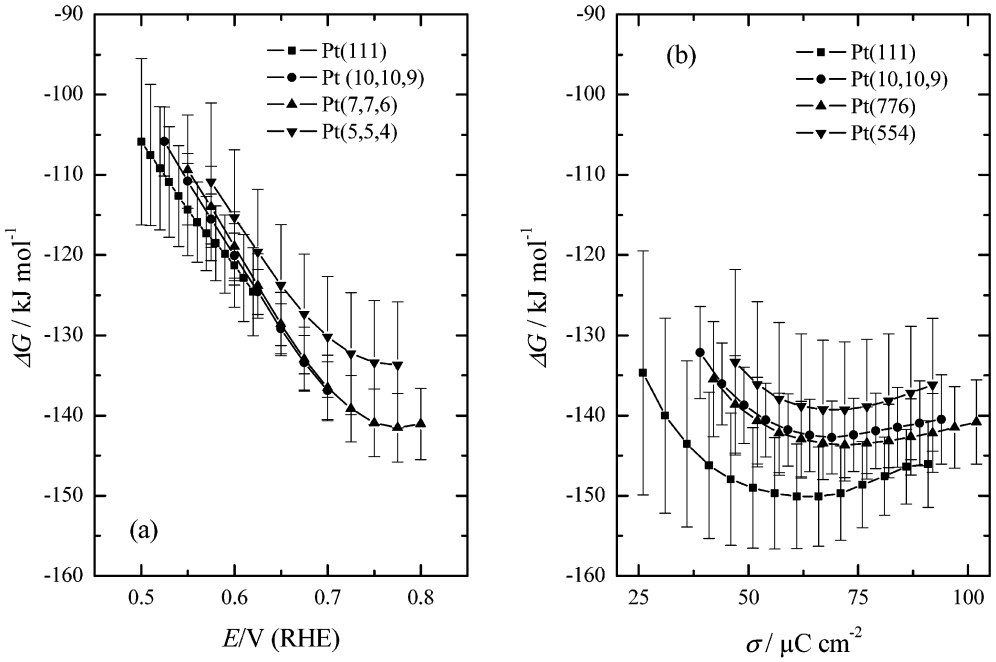

Figure 10. Gibbs energy of adsorption Δ*G* vs *E* from analysis at (a) constant potential and (b) constant charge, for the various Pt surfaces studied.

at the maximum coverage of adsorbed anion. The differences between the position of minimum on the Gibbs energy plots and the maximum on the surface pressure plots are within the uncertainty of the method used to calculate the Gibbs energies. Overall, the Gibbs energy plots shown in Figures 10a and 10b demonstrate that the absolute value of the Gibbs energy of adsorption systematically decreases when the step density increases.

3.4. Charge Numbers per Adsorbed Anion. The presence or absence of systematic errors in the thermodynamic data processing may be conveniently verified with the help of cross differential equations. Cross differentiation of the electrocapillary equation gives two equations that relate the rate of change of the Gibbs energy of adsorption with the electrical variable to the rate with which charge changes with coverage:[26]

$$\gamma' = -\frac{1}{F}\left(\frac{\partial\sigma}{\partial\Gamma}\right)_E = \frac{1}{F}\left(\frac{\partial\mu}{\partial E}\right)_\Gamma \tag{5}$$

and

$$n' = -\frac{1}{F}\left(\frac{\partial\sigma}{\partial\Gamma}\right)_\mu = \frac{1}{F}\left(\frac{\partial\mu}{\partial E}\right)_\sigma \tag{6}$$

Incidentally, eqs 5 and 6 may also be used to determine γ', the charge number at a constant electrode potential, usually known as electrosorption valency (IUPAC recommends symbol *l* and the name "formal partial charge number" [27]) and n' the charge

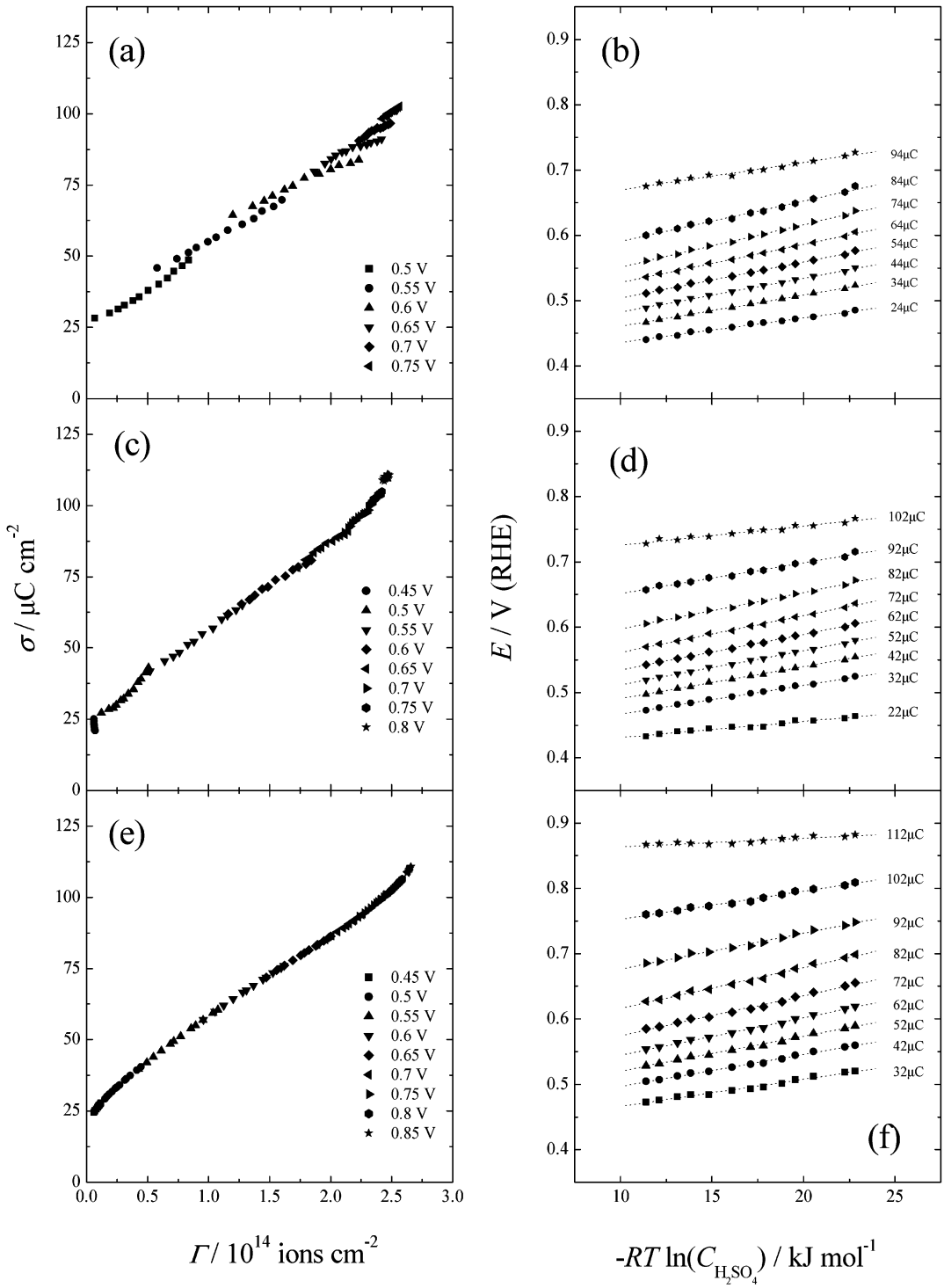

Figure 11. σ vs Γ_- and E vs $RT \ln c_{H_2SO_4}$ plots for the (a,b) Pt(10,10,9), (c,d) Pt(7,7,6), and (e,f) Pt(5,5,4) electrodes.

number at a constant chemical potential that is equal to the reciprocal of the Esin−Markov coefficient.

For the Pt(10,10,9) surface, Figure 11a shows a plot of σ vs Γ_- for various electrode potentials in the region 0.5−0.7 V (RHE). The data display a linear relation between σ and Γ_-. At higher potentials only a very narrow range of Gibbs excesses was available, and hence the linearity of the plots was assumed. The fact that the plots should include σ values measured in the pure supporting electrolyte (when $\Gamma_- = 0$), reduced somewhat the uncertainty about their slopes. Consistent with eq 5, the slope of these plots gives the electrosorption valency. Figure 11b shows a plot of E vs $-RT \ln c_{H_2SO_4}$ for various electrode charge densities in the range from 24 to 94 μC cm^{-2}. The plots are linear and accordingly with eq 6 their slopes give the Esin−Markov coefficients.

The electrosorption valencies calculated from the slopes of the σ vs Γ_- plots are plotted in Figure 12a. In addition, the ΔG values plotted vs E in Figure 10a were fitted to a polynomial and their derivative was determined. The results are also plotted in Figure 12a. The agreement between the values of γ' determined by the two procedures is acceptable and indicates that the Gibbs energies at constant E may be trusted. In addition, the charge numbers at constant chemical potentials were calculated from the slope of the E vs $-RT \ln c_{H_2SO_4}$ at constant

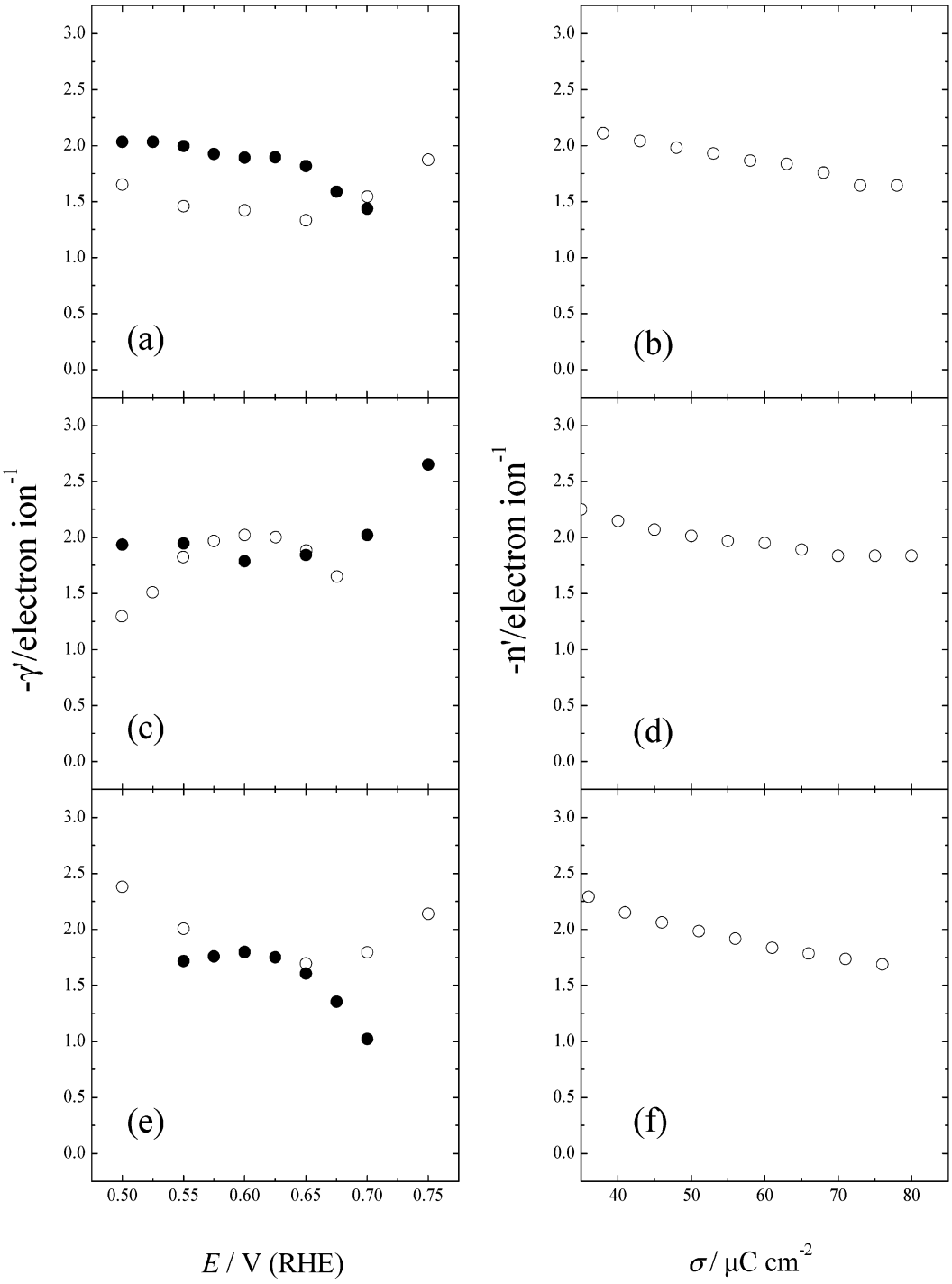

Figure 12. (○) Charge numbers at constant potential (a,c,e) and at constant charge (b,d,f) and (●) the first derivative of the ΔG vs E plots for the Pt(10,10,9) (a,b), Pt(7,7,6) (c,d), and Pt(5,5,4) (e,f) surfaces.

charge. They are plotted against the charge density in Figure 12b. In general, the charge numbers at constant potential or at constant composition of the electrolyte are close to 2 for the three vicinal surfaces and for the Pt(111) surface. We have concluded in our previous paper[16] that this number might be interpreted either as preferential adsorption of sulfate in absence of competitive adsorption or as mixed adsorption of bisulfate and other ions present in the electrolyte.

Conclusions

We have investigated (bi)sulfate adsorption at three stepped surfaces with terraces that were 20, 14, and 10 atoms wide. They were vicinal to the Pt(111) plane. The order−disorder phase transition, observed at the Pt(111) electrode, was not observed at the vicinal surfaces. Apparently, the correlation length for the ordered state is longer than the width of a 20 Pt atoms wide terrace and the disordered state dominates at the stepped surfaces. We have determined surface Gibbs excess for (bi)sulfate, its Gibbs energy of adsorption, electrosorption valency, and Esin−Markov coefficient. The Gibbs excesses at constant potential decrease with the step density at the electrode surface. When the same data are analyzed at constant charge, the effect of surface crystallography is seen only at high surface coverages. This behavior suggests that differences between

adsorption at the Pt(111) and the vicinal surfaces are chiefly due to the formation of the ordered phase at the surface with long (111) terraces. However, the surface pressure and Gibbs energy data show clearly that the energy of (bi)sulfate adsorption decreases with the step density at the surface. This behavior indicates that even in disordered state, (bi)sulfate is preferentially adsorbed at terraces rather than at steps. The charge numbers per adsorbed (bi)sulfate at constant potential and constant composition of the electrolyte are close to ~2 for both Pt(111) and the vicinal surfaces. However, due to the competitive character of the sulfate/bisulfate adsorption these numbers should not be used to determine the nature of the predominantly adsorbed anion.

Acknowledgment. Financial support from MCyT (Spain) (Project BQU2000-0240) is greatly acknowledged. J.M. and J.L. acknowledge the MECD (Spain) and Generalitat Valenciana, respectively, for Visiting Professorships.

References and Notes

(1) Gomez, R.; Orts, J. M.; Feliu, J. M.; Clavilier, J.; Klein, L. H. *J. Electroanal. Chem.* **1997**, *432*, 1.

(2) Lebedeva, N. P.; Koper, M. T. M.; Feliu, J. M.; Santen, R. A. v. *J. Phys. Chem. B* **2002**, *106*, 9863.

(3) Al-Akl, A.; Attard, G. A.; Price, R.; Timothy, B. *J. Electroanal. Chem.* **1999**, *467*, 60.

(4) Markovic, N. M.; Grgur, B. N.; Lucas, C. A.; Ross, P. N. *Surf. Sci.* **1997**, *384*, L805.

(5) Clavilier, J.; El Achi, K.; Petit, M.; Rodes, A.; Zamakhchari, M. A. *J. Electroanal. Chem. Interfacial Electrochem.* **1990**, *295*, 333.

(6) Kibler, L. A.; Cuesta, A.; Kleinert, M.; Kolb, D. M. *J. Electroanal. Chem.* **2000**, *484*, 73.

(7) Gomez, R.; Feliu, J. M.; Abruna, H. D. *J. Phys. Chem.* **1994**, *98*, 5514.

(8) Alvarez, B.; Feliu, J. M.; Clavilier, J. *Electrochem. Commun.* **2002**, *4*, 379.

(9) Jaaf-Golze, K. A.; Kolb, D. M.; Scherson, D. *J. Electroanal. Chem. Interfacial Electrochem.* **1986**, *200*, 353.

(10) Motoo, S.; Furuya, N. *Ber. Bunsen-Ges. Phys. Chem.* **1987**, *91*, 457−461.

(11) Clavilier, J.; Achi, K. E.; Rodes, A. *Chem. Phys.* **1990**, *141*, 1.

(12) Rodes, A.; El Achi, K.; Zamakhchari, M. A.; Clavilier, J. *J. Electroanal. Chem. Interfacial Electrochem.* **1990**, *284*, 245.

(13) Markovic, N. M.; Marinkovic, N. S.; Adzic, R. R. *J. Electroanal. Chem. Interfacial Electrochem.* **1988**, *241*, 309.

(14) Herrero, E.; Orts, J. M.; Aldaz, A.; Feliu, J. M. *Surf. Sci.* **1999**, *440*, 259.

(15) Gomez, R.; Climent, V.; Feliu, J. M.; Weaver, M. J. *J. Phys. Chem. B* **2000**, *104*, 597.

(16) Herrero, E.; Mostany, J.; Feliu, J. M.; Lipkowski, J. *J. Electroanal. Chem.* **2002**, *534*, 79.

(17) Ross, P. N. *J. Chim. Phys.* **1991**, *88*, 1353.

(18) Herrero, E.; Climent, V.; Feliu, J. M. *Electrochem. Commun.* **2000**, *2*, 636.

(19) Clavilier, J.; El Achi, K.; Rodes, A. *J. Electroanal. Chem. Interfacial Electrochem.* **1989**, *272*, 253.

(20) Clavilier, J.; Rodes, A.; El Achi, K.; Zamakhchari, M. A. *J. Chim. Phys. Phys.-Chim. Biol.* **1991**, *88*, 1291.

(21) Climent, V.; Gomez, R.; Feliu, J. M. *Electrochim. Acta* **1999**, *45*, 629.

(22) (a) Shi, Z.; Lipkowski, J.; Mirwald, S.; Pettinger, B. *J. Electroanal. Chem.* **1995**, *396*, 115. (b) Shi, Z.; Lipkowski, J.; Gamboa, M.; Zelenay, P.; Wieckowski, A. *J. Electroanal. Chem.* **1994**, *366*, 317.

(23) Parsons, R. *Proc. R. Soc. (London)* **1961**, *A261*, 79.

(24) Savich, W.; Sun, S.-G.; Lipkowski, J.; Wieckowski, A. *J. Electroanal. Chem.* **1995**, *388*, 233.

(25) Parsons, R. *Trans. Faraday Soc.* **1955**, *51*, 1518.

(26) Delahay, P. *Double layer and electrode kinetics*; Wiley: New York, 1961.

(27) Parsons, R.; Trasatti, S. *J. Electroanal. Chem.* **1986**, *205*, 359.